Supporting Information for

Structural and Mechanistic Basis for the High Activity of Iron-Nitrogen-Carbon Electrocatalysts toward Oxygen Reduction

Jingkun Li[a], Shraboni Ghoshal[a], Wentao Liang[b], Moulay-Tahar Sougrati[c], Frederic Jaouen[c], Barr Halevi[d], Samuel McKinney[d], Geoff McCool[d], Chunrong Ma[e], Xianxia Yuan[e], Zi-Feng Ma[e], Sanjeev Mukerjee[a,*], and Qingying Jia[a,*]

[a] Department of Chemistry and Chemical Biology, Northeastern University, Boston, Massachusetts, 02115, United States

[b] Department of Biology, Northeastern University, Boston, Massachusetts 02115, United States

[c] Institut Charles Gerhardt Montpellier, UMR CNRS 5253, Université Montpellier, Agrégats, Interfaces et Matériaux pour l'Energie, Montpellier, 34095, France

[d] Pajarito Powder, LLC (PPC), Albuquerque, New Mexico 87102, , United States

[e] Shanghai Electrochemical Energy Devices Research Center, Department of Chemical Engineering, Shanghai Jiao Tong University, Shanghai 200240, People's Republic of China

* To whom correspondence should be addressed. E-mail: s.mukerjee@neu.edu, Q.jia@neu.edu.

X-ray Absorption Spectroscopy (XAS) data collection and Analysis. The electrode inks for the XAS electrodes were composed of 1:3 (wt%) 18.2 MΩ purity deionized water (Millipore) and 2-propanol (HPLC-grade, Aldrich), a 5 wt% Nafion solution (Aldrich), and the catalyst powder. The composition was chosen to give a final electrode with a dry Nafion loading of 5 wt%. The inks were directly sprayed onto a Zoltek® carbon cloth on a piece of heated glass. The final Fe loading is ~0.05 mg_{Fe} cm^{-2} in the electrodes (1×3 cm^2). *Ex situ* XAS data were firstly collected on the dry electrodes, which were then conditioned in 0.1 M $HClO_4$ under vacuum for three hours to remove the oxides, impurities, and gases trapped inside the electrode, and to wet the electrodes (the electrodes were not thoroughly wet due to the high hydrophobicity). Afterwards, the electrodes were further conditioned electrochemically in the flow cell for 50 cycles between 0.05 and 1.05 V with a scan rate of 50 mV s^{-1} in N_2-saturated 0.1 M $HClO_4$ electrolyte. Full range Fe K-edge spectra were taken at various static potentials along the anodic sweep of the cyclic voltammetry (CV) in N_2 or O_2-saturated 0.1 M $HClO_4$ electrolyte. Data were collected in fluorescence mode with a Fe reference foil positioned between I2 and I3 as a reference. The voltage cycling limits were 0.05 to 1.05 V vs. RHE. Data collection was performed at the chosen potentials held during anodic sweeps. Before each measurement, the cell was held for 5 minutes to reach a pseudo-steady state. The electrodes were fully cycled following each potential hold in order to clean the catalyst surfaces after each potential hold.

Scans were calibrated, aligned and normalized with background removed using the

IFEFFIT suite.[1] The data was processed and fitted using the Athena[1] and Artemis[2] programs. The χ(R) transforms were modeled using scattering paths calculated by the FEFF6 code.[3] Data analysis for Delta−Mu (Δμ) studies at the Fe K−edge involved specific normalization procedures detailed elsewhere.[4] Difference spectra were obtained using the equation

$$\Delta\mu = \mu(V, N_2 \text{ or } O_2) - \mu(0.1\ V, N_2) \quad (1)$$

where μ(V, N_2 or O_2) is the XANES of the catalyst at various potentials in N_2- or O_2-saturated electrolyte, and μ(0.1 V, N_2) is the reference XANES signal at 0.1 V in N_2-saturated electrolyte at which potential no evidence for electrochemical adsorbates (H*, O(H)*) were found on these iron-based catalysts. Theoretical delta mu curves ($\Delta\mu_t$) were constructed using the FEFF9 code.[5] This was accomplished using the relationship

$$\Delta\mu_t = \mu(O_{ads}\text{-Fe-}N_x\text{-C}) - \mu(\text{Fe-}N_x\text{-C}) \quad (2)$$

where the oxide species (O_{ads} or $O(H)_{ads}$) is in the axial binding site on Fe. It is noted that O_{ads} and OH_{ads} can not be difficientiated by Δμ.

Detailed scale up procedure of FePhenMOF-ArNH$_3$. A near linear scale up was developed where 16.282g of calcined (400°C) zinc oxide, 32.832g of 2-methylimidazole, and 1.057g of ammonium sulfate were well mixed in a 600mL polypropylene milling jar with 96 ø6mm pieces and 4 ø10mm pieces of agate milling media. A solution of isopropanol, water, and surfactant with respective volumes of 8 mL/1.421 mL/0.142 mL was added to the dry powder mixture and milled in a planetary ball mill (Across International, #PQ-N4) to make the MOF precursor. Isopropanol was used because it is

less toxic than methanol; water was used to help solubilizing the ammonium sulfate, and a surfactant was used to lower the surface energy between the particles to reduce clumping. Such adjustments in the recipe were made for manufacturing at larger scale, with costs, ease of handling, and processing robustness taken into account. The MOF precursor, 1,10-phenanthroline, and stabilized iron salt with a mass ratio of 80:20:1 (MOF:Phenanthroline:Fe) are further milled and the resulting coral colored powder was subjected to the double heat treatments. Because of the larger furnaces utilized in the scaled-up process, the temperatures for thermal treatments were adjusted according to the actual temperatures measured within the processing tubes. The yield of the two heat treatments for scaled-up approach was approximately 20%.

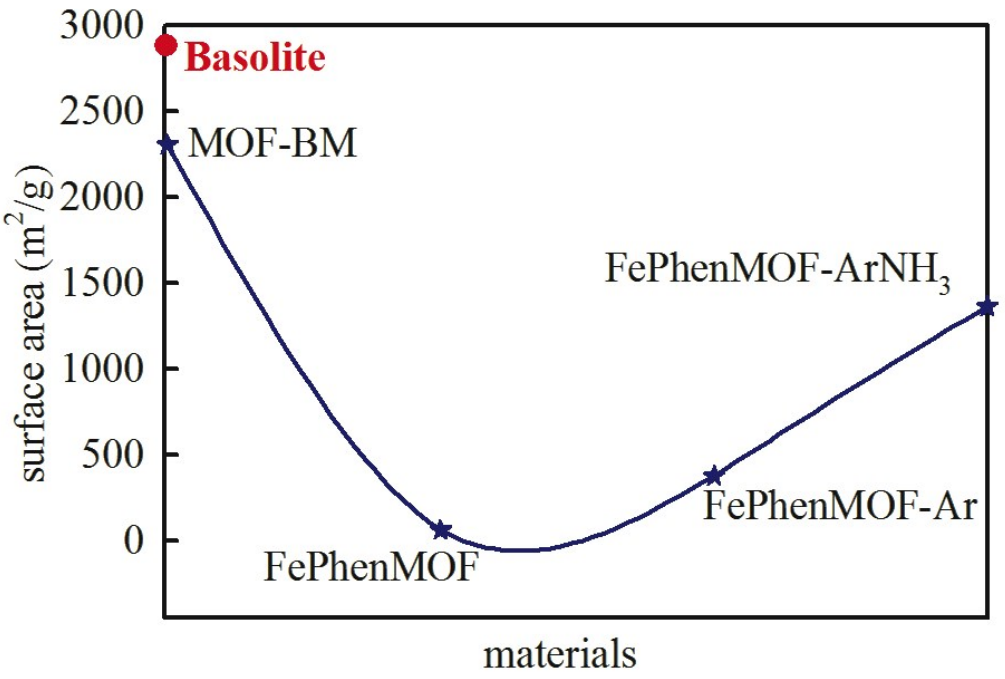

Figure S1. Brunauer-Emmett-Teller (BET) surface area of non-heat treated Basolite Z1200®, MOF synthesized through reactive ball milling approach, FePhenMOF, FePhenMOF-Ar and FePhenMOF-$ArNH_3$. The BET surface area of house-synthesized MOF is similar comparing to that of the commercial Basolite Z1200®. The drastically

diminish of BET surface area of FePhenMOF is due to the blocking of the pores by phenanthroline, and the surface area is recovered upon heat treatments.

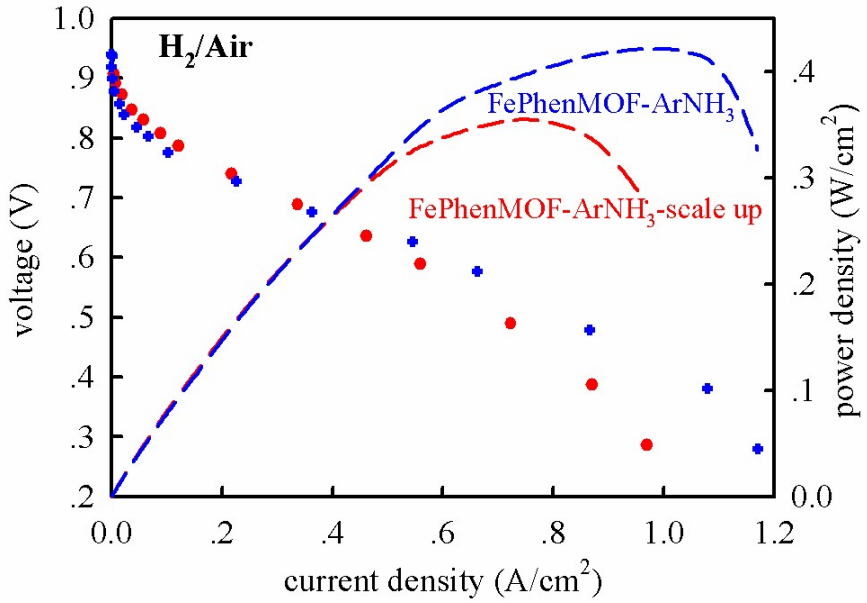

Figure S2. H_2/air fuel cell polarization curves and corresponding power density curves for same MEA collected with FePhenMOF-$ArNH_3$ and FePhenMOF-$ArNH_3$-scale up (by 20 times). The fuel cell was operated at 80 °C under a feed 200 sccm of 90% RH air and H_2 and 2 bar back pressure with a loading of 2 mg cm^{-2} catalyst at cathode and 0.1 mg cm^{-2} Pt at anode.

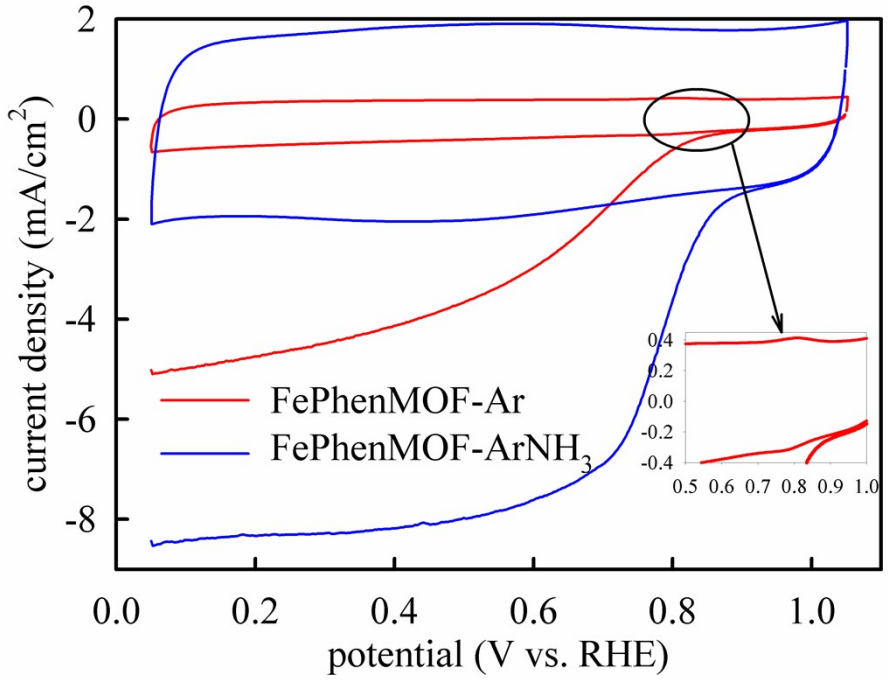

Figure S3. Cyclic voltammogram (CV) plots collected with FePhenMOF-$ArNH_3$ and FePhenMOF-Ar with identical catalyst loading in Ar-saturated 0.1 M $HClO_4$ electrolyte at 20 mVs^{-1} at room temperature, together with the ORR polarization ORR polarization plots collected with FePhenMOF-$ArNH_3$ and FePhenMOF-Ar in O_2-saturated 0.1 M $HClO_4$ electrolyte at 20 mVs^{-1} with rotation rate of 1,600 r.p.m. at room temperature.

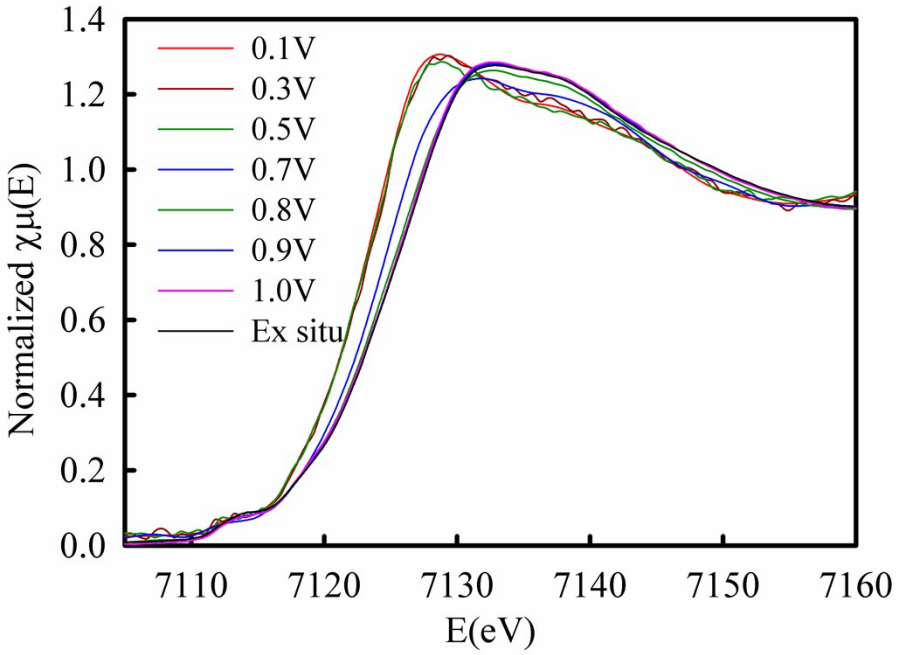

Figure S4. *Ex situ* and *in situ* XANES of the FePhenMOF-$ArNH_3$ catalyst. *Ex situ* data were firstly collected on the dry electrode, and the *in situ* spectra were collected at 0.1-1.0 V on the same electrode in O_2/N_2-saturated 0.1 M $HClO_4$ at room temperature.

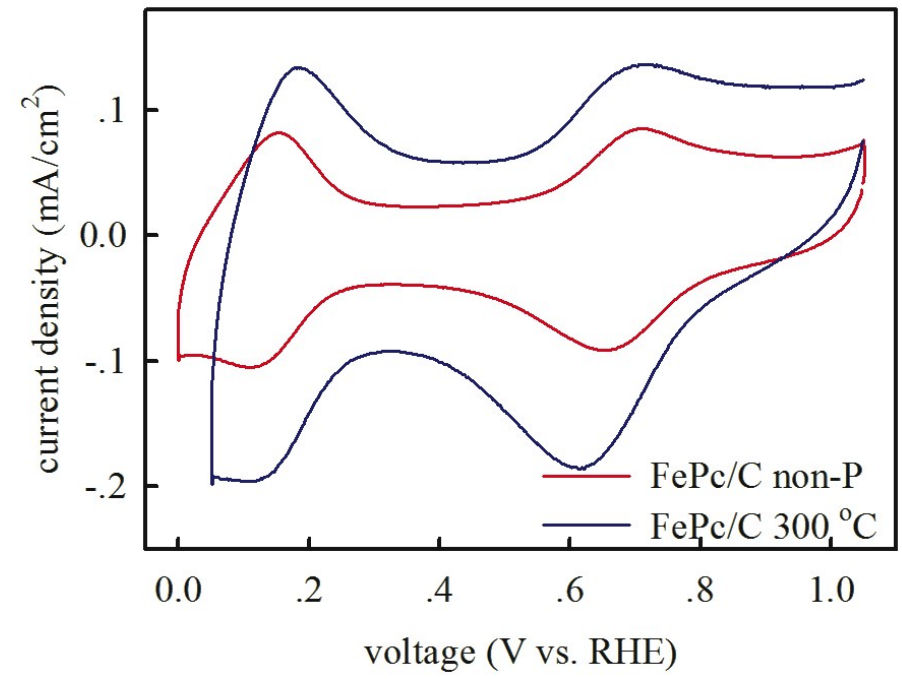

Figure S5. Cyclic voltammogram (CV) plots collected with FePc/C (non-pyrolyzed) and FePc/C (300 °C) in N_2-saturated 0.1 M $HClO_4$ electrolyte at 20 mV s^{-1} at room temperature. Both of them have shown a redox peak at around 0.64 V vs. RHE, which is attributed to the $Fe^{2+/3+}$ redox of the D2 site.

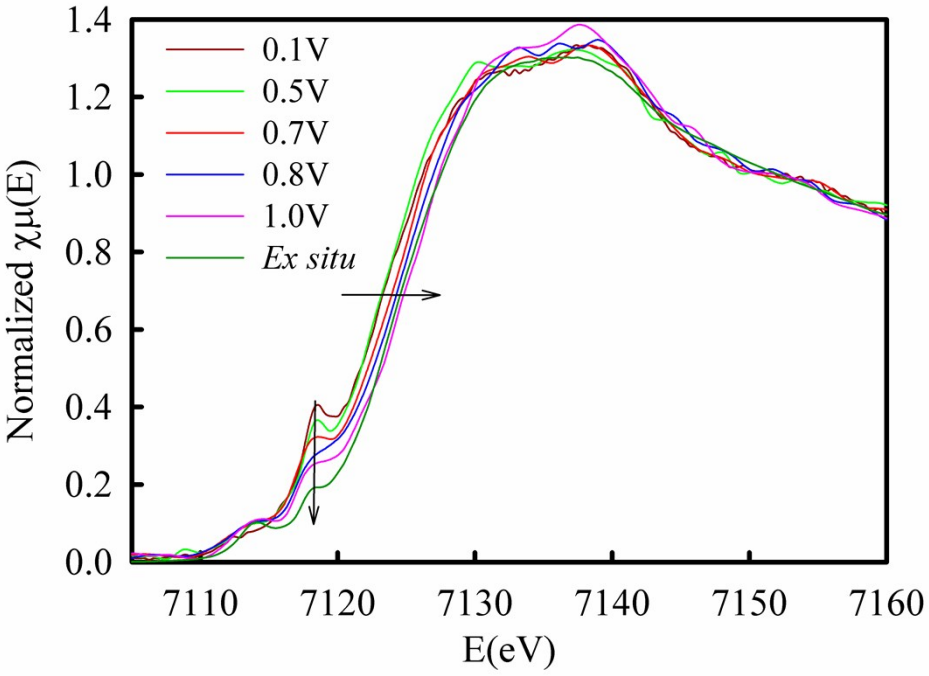

Figure S6. *Ex situ* and *in situ* XANES of the FePc/C pyrolyzed at 300 °C. *Ex situ* data were firstly collected on the dry electrode, and the *in situ* spectra were collected at 0.1-1.0

V on the same electrode in O_2/N_2-saturated 0.1 M $HClO_4$ at room temperature.

Table S1. Gravimetric double layer capacitance (*C*), effective electrochemical surface area (S_a) and Brunauer-Emmett-Teller (BET) surface area of FePhenMOF-Ar and FePhenMOF-$ArNH_3$.

	C (F mg^{-1})	S_a (m^2 g^{-1})	Total surface area (m^2 g^{-1})	Micropore surface area (m^2 g^{-1})	Mesopore surface area (m^2 g^{-1})
FePhenMOF-Ar	0.03	167	378	115	263
FePhenMOF-$ArNH_3$	0.17	833	1362	872	490

The gravimetric double layer capacitance (*C*, F mg^{-1}) is estimated according to: $(I_a-I_c)/(2\times L_{catalyst})= C\times(dE/dt)$, where I_a and I_c are the anodic and cathodic current density extracted from CVs in Ar at the potential without any Faradic process.[6] The electrochemical surface area (S_a) values are calculated from the double layer capacitance using 0.2 F m^{-2} as the "unit" capacitance of carbon-based catalysts.[6] The total surface area is determined by the Brunauer-Emmett-Teller (BET) analysis of the corresponding N2 adsorption isotherms. Micropores are defined as pores with widths < 2 nm, while mesopres are pores with widths between 2 and 50 nm; the widths of macropores are >50 nm.

Table S2. Surface elemental composition of FePhenMOF-$ArNH_3$ as determined by XPS.

	C	O	N	Fe
Atomic %	90.24	3.93	5.31	0.51
Weight %	86.72	5.03	5.95	2.29

Table S3: Results of fitting EXAFS data obtained under *ex situ* and *in situ* electrochemical operating conditions for indicated catalysts. *In situ* experiments performed at the Fe K-edge as a function of potential in O_2−saturated 0.1 M $HClO_4$ electrolyte. Coordination number (N) and phase-corrected bond length (R) are shown for each interaction. Also shown are the Debye-Waller factor (σ^2) and edge shifts (E_0).[a]

FePhenMOF-$ArNH_3$	$N_{Fe-N/O}$[b]	$R_{Fe-N/O}$ (Å)[b]	$\sigma^2 \times 10^{-3}$ (Å^2)	E_o (eV)
0.1 V	3.8±0.6	2.07±0.02	6±3	-4.1±2.1
1.0 V	5.4±1.3	1.99±0.03	4±2	1.5±1.4
Ex situ	5.3±0.5	1.99±0.01	4±1	1.3±0.6

[a]S_0^2 fixed at 0.88 as obtained by fitting the reference foil. The Fourier−transformed (FT) EXAFS data were fitted under simultaneous $k^{1,2,3}$ weighting. The statistical errors of the

least-squares fits were determined by ARTEMIS. The fitting parameters and the R values are given in Table S4. [b]N and O cannot be distinguished by XAS as surrounding atoms.

Table S4: Summary of the EXAFS fitting parameters used for the EXAFS fits listed in Table S3 and the R values.

	k range [Å^{-1}]	R range [Å]	R factor
0.1 V	1.95-9.92	1.0-2.6	0.023
1.0 V	2.02-9.92	1.0-2.6	0.021
Ex situ	2.02-10.90	1.0-2.6	0.011

Table S5. Comparison of the metal loadings, loadings of D1 sites, kinetic current densities and estimated turn-over frequencies (TOF) of the catalysts described in this work with those reported previously.[7-9]

	Fe/wt %	Fe(D1)/wt %	J(0.8 V)/A g_{cat}^{-1}	TOF(0.8 V)/ e s^{-1} $sites^{-1}$
FePhenMOF-ArNH_3	0.5	0.20	7.78	2.40
$(Fe,Fe)_1$[7]	3.1	1.25	0.45	0.02
$(Fe,Fe)_1$+N_2/H_2[7]	2.4	1.20	1.23	0.06
0.5Fe[8]	1.5	0.75	1.47	0.11
0.5Fe-900[8]	1.2	0.60	3.42	0.33
Fe-N-C-3HT-2AL[9]	6.0	1.33	21.0	0.93
(Fe,Mn)-N-C-3HT-2AL[9]	3.0	1.17	17.6	0.87

The Fe loading of FePhenMOF-ArNH_3 is measured by inductively coupled plasma mass spectrometry (ICP-MS), and the loading of D1 site ($c_{Fe,D1}$) is calculated based on the absorption area of the doublets D1 obtained through Mössbauer spectroscopy. The mass based kinetic current density of FePhenMOF-ArNH_3 at 0.8 V versus RHE is estimated according to: $I_{kin,0.8V}=I_{0.8V}\times I_{lim}/((I_{lim}-I_{0.8V})\times L_{catalyst})$, using the current density at 0.8 V measured in O_2-saturated 0.1 M $HClO_4$ electrolyte at 20 mV s^{-1} with rotation rate of 1,600 r.p.m., the diffusion limited current density I_{lim} and the catalyst loading $L_{catalyst}$ (600 μg cm^{-2}). The Fe loadings, loadings of D1 sites and kinetic current densities of $(Fe,Fe)_1$, $(Fe,Fe)_1$+N_2/H_2, 0.5Fe and 0.5Fe-900 are obtained from Ref. 7. The Fe loadings, loadings of D1 sites and kinetic current densities of Fe-N-C-3HT-2A and (Fe,Mn)-N-C-3HT-2AL are extracted from Ref. 9. The turn-over frequency (TOF) at 0.8 V versus RHE is estimated following the method introduced in Ref 7 for comparison purposes: TOF (0.8 V)=$100\times M_{Fe}\times I_{kin,0.8V}/(c_{Fe,D1}\times N_A\times e^-)$, where M_{Fe} is the molecular weight of Fe (55.845 g mol^{-1}), N_A is the Avogadro constant (6.02×10^{23} mol^{-1}), and e^- is the charge of an electron (1.602×10^{-19} C).

References

(1) Newville, M. *J. Synchrotron. Radiat.* **2001**, *8*, 322.

(2) Ravel, B.; Gallagher, K. *Phys. Scr.* **2005**, *T115*, 606.

(3) Zabinsky, S. I.; Rehr, J. J.; Ankudinov, A.; Albers, R. C.; Eller, M. J. *Phys. Rev. B.* **1995**, *52*, 2995.

(4) Roth, C.; Benker, N.; Buhrmester, T.; Mazurek, M.; Loster, M.; Fuess, H.; Koningsberger, D. C.; Ramaker, D. E. *J. Am. Chem. Soc.* **2005**, *127*, 14607.

(5) Ankudinov, A. L.; Ravel, B.; Rehr, J. J.; Conradson, S. D. *Phys. Rev. B Condens. Matter Mater. Phys.* **1998**, *58*, 7565.

(6) Zhou, Y.-k.; He, B.-l.; Zhou, W.-j.; Huang, J.; Li, X.-h.; Wu, B.; Li, H.-l. *Electrochim. Acta* **2004**, *49*, 257.

(7) Kramm, U. I.; Herrmann-Geppert, I.; Behrends, J.; Lips, K.; Fiechter, S.; Bogdanoff, P. *J. Am. Chem. Soc.* **2016**, *138*, 635.

(8) Zitolo, A.; Goellner, V.; Armel, V.; Sougrati, M.-T.; Mineva, T.; Stievano, L.; Fonda, E.; Jaouen, F. *Nat. Mater.* **2015**, *14*, 937.

(9) Sahraie, N. R.; Kramm, U. I.; Steinberg, J.; Zhang, Y.; Thomas, A.; Reier, T.; Paraknowitsch, J.-P.; Strasser, P. *Nat. Commun.* **2015**, *6*.